Accepted Manuscript

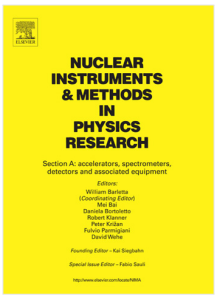

Operational properties of fine powder aerosol as radiation detection medium in gaseous proportional counters

N.F.V. Duarte, C.M.B. Monteiro, C.D.R. Azevedo, A. Antognini, F.D. Amaro

PII: S0168-9002(19)30974-X
DOI: https://doi.org/10.1016/j.nima.2019.162392
Article number: 162392
Reference: NIMA 162392

To appear in: *Nuclear Inst. and Methods in Physics Research, A*

Received date : 14 December 2018
Revised date : 28 June 2019
Accepted date : 15 July 2019

Please cite this article as: N.F.V. Duarte, C.M.B. Monteiro, C.D.R. Azevedo et al., Operational properties of fine powder aerosol as radiation detection medium in gaseous proportional counters, *Nuclear Inst. and Methods in Physics Research, A* (2019), https://doi.org/10.1016/j.nima.2019.162392

Operational properties of fine powder aerosol as radiation detection medium in gaseous proportional counters

N.F.V. Duarte[a], C.M.B. Monteiro[a], C.D.R. Azevedo[b], A. Antognini[c,d], F. D. Amaro[a,*]

[a] *LIBPhys - Physics Department, University of Coimbra, 3004-516 Coimbra, Portugal*
[b] *I3N - Physics Department, University of Aveiro, 3810-193 Aveiro, Portugal*
[c] *Institute for Particle Physics and Astrophysics, ETH Zurich, 8093 Zurich, Switzerland*
[d] *Paul Scherrer Institute, 5232 Villigen, Switzerland*

Abstract

Due to its exceptional properties, ^{3}He proportional counters are the golden standard for neutron detection, particularly in homeland security applications where large area detectors are deployed. However, in recent years ^{3}He has become severely scarce, which led to a tremendous price increase and acquisition restrictions of this material. Motivated by this, the development of ^{3}He-free solutions became a priority. In a previous work, we have established a novel concept for neutron detection: a proportional counter with boron carbide (B_4C) fine powder suspended in the proportional gas forming a neutron sensitive aerosol that relies on the ^{10}B neutron capture reaction. Computer simulations and prototype exposure to a cold neutron beam yielded favorable results, validating the detection concept, which may also be applied to hard x-ray and gamma ray detection by using fine particles made of a heavy element, such as Bi or Au. In this work we study the effect of the presence of B_4C microparticles in the charge gain and energy resolution of a proportional counter filled with Ar-CH_4 (90%-10%), by irradiation with x-rays from a ^{55}Fe source. For the same applied voltage, an average gain loss by a factor of 36% and energy resolution (FWHM) increase by 15% (absolute value) was observed with the inclusion of B_4C microparticles. Intrinsic energy resolution was calculated, obtaining 15% for pure P10 operation and 32% in the presence of the microparticles. While the gain drop is recoverable by increasing anode voltage, energy resolution degradation may be a drawback in low energy applications, were energy resolution is favored over detection efficiency.

Keywords: Proportional counter, Neutron detection, Gamma ray detection, ^{10}B, ^{3}He alternative.

* Corresponding author.
E-mail address: famaro@gian.fis.uc.pt

1. Introduction

1.1. The ^{3}He shortage crises

Neutron detectors are used in a wide range of applications, with the main consumers being homeland security instruments, such as Radiation Portal Monitors (RPMs) and handheld or backpack radiation monitoring systems. The ^{3}He gaseous proportional counter is the most common neutron detector deployed, due to its excellent detection efficiency, good gamma-ray discrimination, non-toxicity and the fact that it can be used to produce large area detectors. However, ^{3}He reserves are in decline which, in association with the great number of RPMs deployed, has led to an unsustainable situation, with the current demand for ^{3}He surpassing its worldwide supply [1-8].

Since the scientific community became aware of the ^{3}He shortage crises, research and development on ^{3}He-free neutron detection solutions became a priority and innovative alternatives are being developed. A variety of techniques have been reported, including boron-lined detectors coupled to multi-wire proportional counters (MWPC) [9,10] and to gas electron multipliers (GEM) [11,12], arrays of boron-coated straws [13-15], aerogel and saturated foam detectors [16-18], scintillators [19,20], suspended lithium foils coupled to MWPC [21-23] and lithium backfilled microstructures [24,25].

This research is heavily restricted by the fact that only a few isotopes have the ability of absorbing neutrons and inducing nuclear capture reactions. In addition, for detection applications, the products of these reactions should comprise exclusively heavy charged particles, rather than gamma-rays or beta radiation. Based on these considerations, the list of alternative isotopes that can be used in neutron detection is narrowed to ^{6}Li and ^{10}B. Among these, ^{10}B has a higher thermal neutron cross-section (3840 barn, versus 940 barn), which implies a greater detection efficiency potential.

1.2. B_4C fine powder aerosol: a novel approach

A novel concept for neutron detection has been proposed in a previous work, which consists on a proportional counter filled with P10 (Ar-CH_4, 90%-10%) in which a boron-based fine powder is dispersed (boron-carbide was used), forming a neutron sensitive aerosol [26]. A detection efficiency of 4% was reported while irradiating a prototype with cold neutrons (5 Å). The boron carbide (B_4C) fine powder is made of natural boron, of which the ^{10}B fraction is approximately 20%. Commercially available ^{10}B enriched boron-carbide fine powder would lead up to a 5-fold increase in detection efficiency.

In this neutron sensitive aerosol detection technique, the B_4C particles are suspended in the proportional gas by an appropriate gas flow which counter-acts the gravity force. As an incoming neutron interacts with the ^{10}B atoms of the microparticles, 2 products are released in opposite directions: a ^{7}Li ion (0.84 MeV) and an α-particle (1.47 MeV). The main benefit of this detection concept is that both reaction products can escape the B_4C particles, since their range in this material is greater than the particles size. This allows for the deposition of a large fraction of the energy released by the neutron capture reaction in the filling gas, resulting in a full energy deposition peak (2.3 MeV) in the pulse height distribution of the detector. This feature is impossible to achieve with alternatives based on boron coating, in which the neutron capture occurs in a solid layer deposited on the walls of the detector. In these alternatives, for each reaction product that reaches the gas volume, the other one is inevitably lost to the detector walls, due to their ejection into opposite directions [27,28]. This leads to a two-step plateau in the pulse height distribution which extends to the low energy region (wall-effect)

and reduces the ability to discriminate between neutron captures and gamma-rays induced events.

The presence of the B_4C fine powder in the proportional counter caused no operational issues, such as electrical discharges or a drastic gain decrease that prevented its operation. Nonetheless, it is essential to understand how the detector is affected by the presence of the fine powder in order to delineate an effective strategy for prototype optimization. The impact of the presence of B_4C particles in the gas gain and energy resolution of the proportional counter are assessed in this work. Tests were performed by irradiating the proportional counter, filled with an aerosol composed by B_4C microparticles dispersed in a P10 atmosphere, by soft x-rays (5.9 keV) from a ^{55}Fe source.

2. Methods

A scheme of the proportional counter used in this work is presented in Fig. 1. It consists of a stainless-steel cylinder with an inner diameter of 47.6 mm and a 50 µm diameter tungsten anode wire stretched along its axis. The anode is electrically insulated from the walls (at ground potential) by ceramic feedthroughs. When a positive voltage is applied to the anode, an electric field is established inside the proportional counter reaching values above the threshold for charge multiplication in a small region around the anode wire. The proportional counter is equipped with a 13 mm diameter window made of a 50 µm thick aluminized Mylar film, glued to the detector with a conductive epoxy. The primary electron clouds resulting from the interaction of x-rays emitted by a ^{55}Fe radioactive source are multiplied through charge avalanche processes around the anode and the resulting charge is collected with a charge sensitive pre-amplifier (Canberra 2006). The pre-amplifier signals are fed to a linear amplifier (Ortec 454), which output is connected to a multichannel analyser.

The proportional gas used was P10, continuously flowing at a rate of 8 l/h. The gas outlet was connected, via a reservoir filled with low outgassing oil, to the atmosphere. The inlet and outlet were equipped with 2 µm filters to prevent the B_4C particles from escaping.

The detector was irradiated with 5.9 keV x-rays from a ^{55}Fe source while the anode voltage was varied from 2000 V to 2400 V. Pulse height distributions were acquired for 60 seconds for each anode voltages, initially without the microparticles inside the detector and subsequently after depositing 3 grams of B_4C fine powder (PlasmaChem GmbH), in the hollow funnel-shaped part of the bottom flange. The method used for particle dispersion in the gas consisted on violently opening the gas flow for a few seconds and subsequently reducing it to 8 l/h, the rate used during

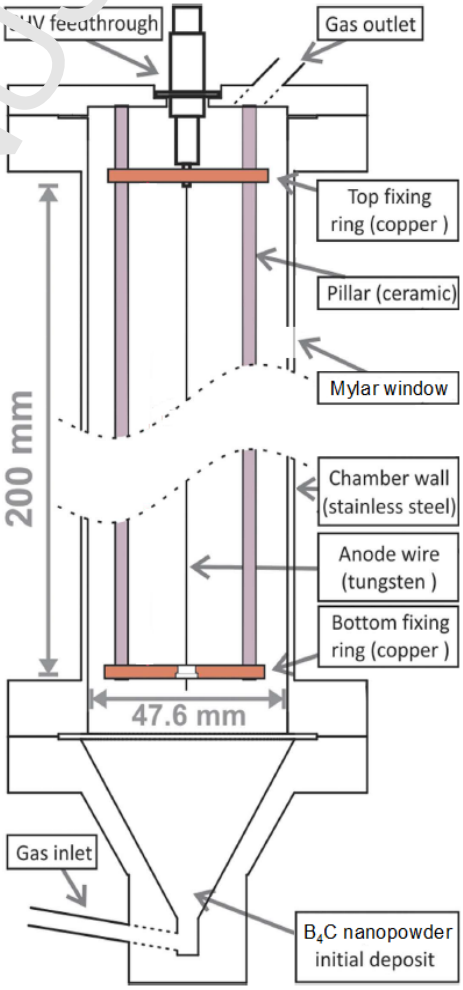

Fig. 1. Schematic of the proportional counter used in this work. Differences from [26] are the removal of the field cage copper wires and the addition of a thin Mylar window.

data acquisition.

A sample of the fine powder used in this work was subject to characterization by laser diffraction (Beckman Coulter LS 13 320). Assuming sphere-like particles, the results yield a mean diameter value of 1.056 µm (d_{10} = 0.553 µm, d_{50} = 1.029 µm and d_{90} = 1.602 µm). It should be noticed that the size characterization was performed using ethanol as the suspension fluid. Despite the use of rollers, magnetic stirrers and tube rotators to assure the suspension of sampled powders, it is impossible to guarantee that the agglomeration behaviour of the particles while suspended in liquid ethanol and in gaseous P10 is identical [29]. In addition, this behaviour also depends on environmental factors such as temperature and humidity. Thus, the 1.056 µm diameter should be considered as nominal value.

3. Results

A comparison of the pulse height distributions recorded for an anode voltage of 2375 V without and with B_4C microparticles in the proportional counter is presented in Fig. 2. Along with the data points, a double peak Gaussian fit is shown for each pulse height distribution. The main peak corresponds to the full absorption of the 5.9 keV x-ray in the proportional gas, while the lower amplitude peak corresponds to the Ka fluorescence escape peak of Ar.

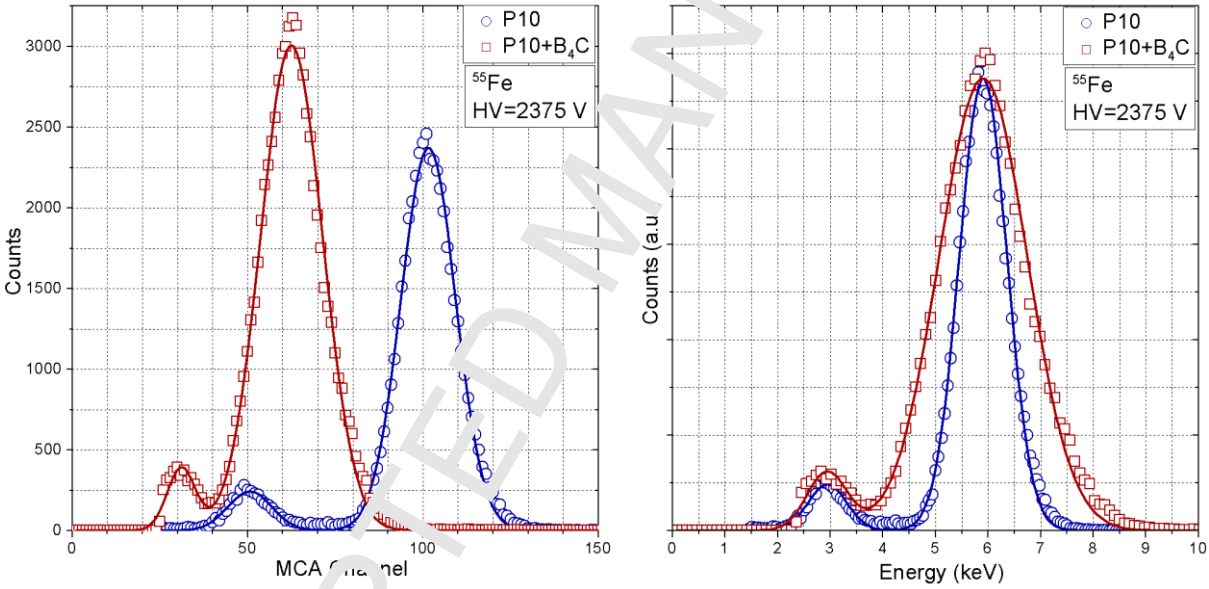

Fig. 2. Pulse height distributions recorded with x-rays irradiation from a ^{55}Fe source and an anode voltage of 2375 V without (blue circles) and with (red squares) B_4C fine powder dispersion. Acquisition time = 60 s. Left: Unnormalized data; Right: Normalization of P10+B_4C data, to match the counts and centroid of the Gaussian fit taken with just P10.

The pulse height distribution is shifted to the lower energy end on the acquisition recorded in the presence of the B_4C particles, which was verified throughout all the anode voltage range. As shown, the presence of the particles suspended in the gas resulted in a lower charge gain achieved by the electron avalanche.

In Fig. 2-right, the pulse height distribution taken with the B_4C microparticle aerosol was normalized in its vertical and horizontal axes so that its amplitude and centroid match the corresponding parameters of the Gaussian fit obtained without the microparticles. The MCA (Multichannel analyzer) axis was also calibrated to the energy scale. A broadening of the 5.9 keV peak after the fine powder dispersion is clearly visible, which implies an energy resolution degradation. This effect was observed for the whole range of applied anode voltages.

Fig. 3 illustrates the gain obtained with and without B_4C microparticles as a function of anode voltage. A gain drop by a factor of 36%, independent of the anode voltage, is observed in the presence of B_4C microparticles. Fig. 3 also suggests that this microparticle induced gain drop can be compensated by increasing the anode voltage by approximately 75 V. A similar analysis was performed for the energy resolution (R). The results, depicted in Fig. 4, show an average degradation of the energy resolution by 15% (absolute value) in the presence of B_4C microparticles, with little dependence on the applied anode voltage.

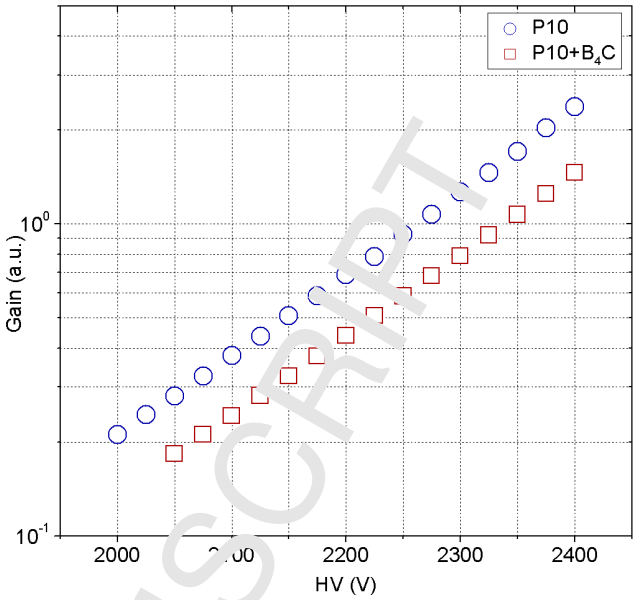

Fig. 3. Logarithmic plot of the gas gain measured for each anode voltage without (blue circles) and with (red squares) B_4C fine powder dispersion. An average gain decrease by a factor of 36% was observed.

The intrinsic energy resolution, a statistical limit associated with the minimum amount of fluctuation that will always be present on the detector signal, arising from the discrete nature of the measured signal itself, was determined for each case. Overlooking electronic noise, which is typically a small contributing factor to the output signal of proportional counters; intrinsic energy resolution can be derived from [30]:

$$R = 2.355 \times \sqrt{\frac{(F+f)}{n_0} + \frac{1}{n_0 \bar{G}}} \qquad (1)$$

where n_0 represents the number of primary ion-electron pairs created by the incident radiation, $\bar{G}$ the average gas gain, F the Fano factor, f the multiplication variance, associated to the relative variance of the number of electrons produced in an avalanche assuming a Polya distribution and 2.355 the ratio between the full width at half maximum of a Gaussian distribution and the standard deviation.

The number of primary ion-electron pairs produced is proportional to the energy deposited by the incident radiation, E_X. The proportionality constant between them is given by w, the mean energy required to form one ion-electron pair (26 eV in argon [30]).

$$n_0 = \frac{E_X}{w} \qquad (2)$$

The intrinsic energy resolution can be experimentally determined by considering the proportionality between the centroids of the 5.9 keV peaks in the pulse height distributions (A) and the detector gain ($\bar{G}$):

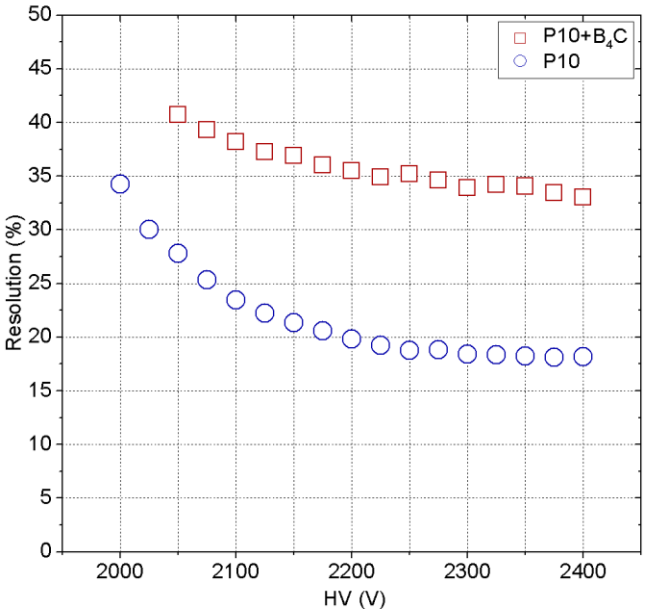

Fig. 4 – Energy resolution of the proportional counter versus applied anode voltage without (blue circles) and with (red squares) B_4C microparticles dispersion. An average energy resolution worsening of 15% (absolute value) was observed when dispersing the B_4C.

$$A \propto n_0 \bar{G} \Longrightarrow A = n_0 \bar{G} K_e \qquad (3)$$

where K_e is a constant exclusively dependent on the electronics chain detector output. After the replacements expressed in equations (2) and (3) we can rewrite equation (1) as:

$$R = 2.355\sqrt{\frac{w\,(F+f)}{E_X} + \frac{K_e}{A}} \Longrightarrow R^2 = 5.545 K_e \frac{1}{A} + 5.545\frac{w\,(F+f)}{E_X} \qquad (4)$$

From equation (4), one can see that if, for the same incident energy (E_X), A is varied throughout a set of acquisitions (accomplished by varying the anode voltage), a linear relation between R^2 and $\frac{1}{A}$ is expected. Thus, a plot of R^2 versus $\frac{1}{A}$ is a reasonable approximation to extrapolate the intrinsic resolution of the detector, corresponding to value of R^2 when $(1/A) \to 0$, i.e. the y-intercept of the function:

$$R_{\text{int}} = 2.355\sqrt{\frac{w \times (F+f)}{E_X}} \qquad (5)$$

Since parameters w, F and f depend exclusively on the filling gas/aerosol, a variation of the $w \times (F + f)$ factor in the presence of the B_4C microparticles is expected and therefore a variation of the intrinsic energy resolution.

Data in Figs. 3 and 4 was processed according to the method above and the results are presented in Fig. 5. The intrinsic energy resolution (R_{int}) obtained when the detector was filled with P10 gas was of 15%, increasing with the microparticles dispersion to 32%. Only the linear region of each R^2 versus $\frac{1}{A}$ curve, limited by the vertical dashed lines in Fig. 5, was considered for fitting. This was because the effects that cause loss of linearity are not contemplated in equation (4), namely fluctuations in the number of primary electrons reaching the avalanche region for low voltages and fluctuations in the electric field due to the spatial positive charge accumulated for high voltages.

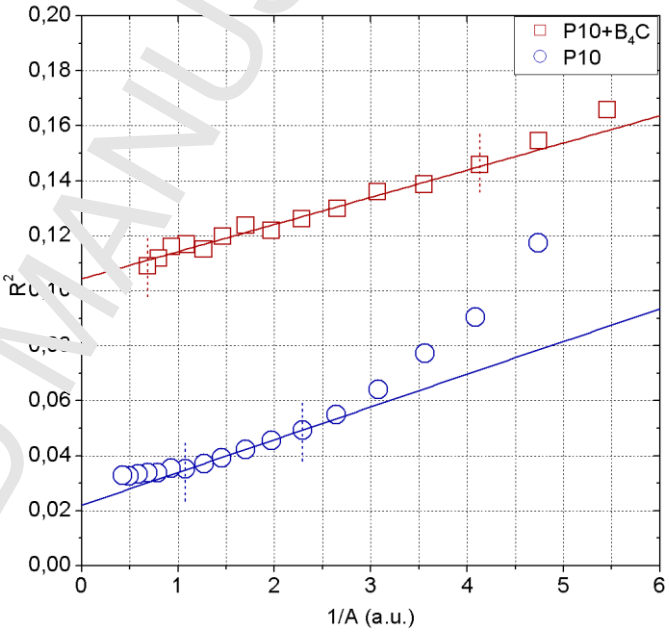

Fig. 5. Square of the energy resolution versus 1/A without (blue circles) and with (red squares) B_4C fine powder dispersion. The extrapolated intrinsic energy resolution values are 15% and 32%, respectively.

As expected the linear portions of the curves are almost parallel, since the slope determined by K_e is similar for both cases.

4. Discussion

One significant concern regarding this detection concept was that dispersing fine powder in a proportional counter could lead to the occurrence of electrical discharges, compromising its operation. In effect, B_4C fine powder was selected in [26] not only for the presence of the

neutron sensitive ^{10}B isotope, but also due to its insulating properties. In this work, the presence of the fine powder did not severely affect the proportional counter by causing discharges or other electrical instabilities during acquisition using soft x-rays.

The microparticles affected however the proportional counter performance, influencing the achievable charge gain and energy resolution. Despite the observed charge gain reduction, the 5.9 keV peak still exhibits a symmetric Gaussian shape (Fig. 2). This indicates that the gain drop is not due to electrons of the avalanches being captured by microparticles. If that were the case, a tail at lower energies would be present on the pulse height distribution as the number of captured electrons would depend on the path travelled.

An analysis of the intrinsic resolution without and with microparticle dispersion provides an insight on the reasons behind the degradation of these parameters. From equation (5) we conclude the factor $w \times (F + f)$ has increased by a factor of 4.8 with the inclusion of the microparticles:

$$\frac{w_{aerosol} \times (F+f)_{aerosol}}{w_{\mathrm{P10}} \times (F+f)_{\mathrm{P10}}} = 4.8 \quad (6)$$

An increase in w due to the inclusion of microparticles is excluded by a pulse height distribution analysis. The discrete nature of the microparticles would cause any process induced by their presence to be also of non-continuous nature, affecting each event according to its degree of interaction with the microparticle. This would create changes in the pulse height distributions, most notably a tail for low energies on the 5.9 keV peak and an increase of the escape peak relative amplitude, which were not present in Fig. 2.

Therefore, we conclude that the increase in the $w \times (F + f)$ factor is due to an increase in the avalanche gain fluctuations $(F + f)$, consequence of the electric field distortion in the region near the microparticle, depending on particle shape and relative orientation to the electric field.

5. Conclusions

The operation of a proportional counter with neutron sensitive B_4C microparticles suspended in P10 gas was studied by irradiation with soft x-rays (5.9 keV). We compared the detector gain, energy resolution and intrinsic energy resolution with and without the dispersion of B_4C microparticles. A gain decrease by a factor of 36% and an energy resolution increase by 15% (absolute value) are observed. Intrinsic energy resolution worsens by approximately 17% (absolute value) in the presence of microparticles.

The degradation of these parameters is justified by the increment of the $w \times (F + f)$ factor, which indicates a rise on the fluctuations in the avalanche charge gain, associated with $(F + f)$, due to inhomogeneities in the electric field created by the microparticles.

It is important to notice that the fine powder did not compromise the detector operation by causing electrical discharges or drastically affecting its charge gain.

This work contributes to the validation of the fine powder aerosol as a radiation detection medium in proportional counters. The detection technique can, in principle, also be used to increase detection efficiency of gaseous detectors to distinct radiation sources. For instance, we can infer that detection of hard x-rays and gamma-rays based on this concept is possible using adequate micro/nanoparticles, made of high Z number materials, such as Bi or Au. While an increase in detection efficiency is expected, it would not come without compromising the achievable gain and energy resolution. The former can be compensated by increasing the electric field, while the later cannot.

Ultimately, the discussed technique is an interesting solution for applications in which detection efficiency is favored over energy resolution. Further tests focusing on hard x-rays/gamma-rays irradiation must be carried to validate of the practicability of this detection technique for application in this energy range. In addition, the buildup of deposits or the development of micro/nanoparticles induced corrosion of the mechanical components will also be evaluated by means of microscope and SEM images of the anode wire, cathode wall and insulator elements, as a function of detector operation time.

Acknowledgments

N.F.V.D. and C.M.B.M. acknowledge the support of FCT, under contracts PD/BD/128268/2016 and SFRH/BPD/76842/2011, respectively. Support is acknowledged under the research project PTDC/NAN-MAT/30178/2017, funded by national funds through FCT/MCTES and co-financed by the European Regional Development Fund (ERDF) through the Portuguese Operational Program for Competitiveness and Internationalization, COMPETE 2020.

References

[1] R.T. Kouzes, The ^{3}He supply problem, Pacific Northwest Natl. Lab. PNNL-18388 (2009). doi:10.2172/956899.
[2] R.T. Kouzes, et. al., Neutron detection alternatives to ^{3}He for national security applications, NIM A 623 (2010) 1035–1045. doi:10.1016/j.nima.2010.08.021.
[3] A.J. Hurd, R.T. Kouzes, Why new neutron detector materials must replace helium-3, Eur. Phys. J. Plus. 129 (2014). doi:10.1140/epjp/i2014-14236-6.
[4] A. Cho, Helium-3 Shortage Could Put Freeze On Low-Temperature Research, Science. 326 (2009) 778–779.
[5] W.K. Hagan, Caught by Surprise: Causes and Consequences of the Helium-3 Supply Crisis, (2009).
[6] T.M. Persons, G. Aloise, Neutron detectors alternatives to using helium-3, GAO-11-753, 2011.
[7] D.A. Shea, D. Morgan, The helium-3 shortage: supply, demand, and options for congress, Congressional Research Service, Library of Congress, 2010.
[8] GAO, Radiation Portal Monitors DHS's Testing is lasting longer than expected, and future acquisitions focus on operational efficiencies, Government Account. Off. (2016) 22.
[9] J. Birch, et. al., $^{10}B_4C$ Multi-Grid as an Alternative to ^{3}He for Large Area Neutron Detectors, IEEE Trans. Nucl. Sci. 60 (2013) 871–878.
[10] F. Piscitelli, Novel boron-10 based detectors for neutron scattering science, Eur. Phys. J. Plus. 130 (2015) 27. doi:10.1140/epjp/i2015-15027-3.
[11] G. Croci, et. al., GEM-based detectors for thermal and fast neutrons, Eur. Phys. J. Plus. 130 (2015). doi:10.1140/epjp/i2015-15110-1.
[12] M. Köhli, et. al., CASCADE-a multi-layer boron-10 neutron detection system, J. Phys. Conf. Ser. 746 (2016). doi:10.1088/1742-6596/746/1/012003.
[13] J.L. Lacy, et. al., Boron coated straw detectors as a replacement for ^{3}He, IEEE Nucl. Sci. Symp. Conf. Rec. (2009) 119–125. doi:10.1109/NSSMIC.2009.5401846.
[14] J.L. Lacy, et. al., The evolution of neutron straw detector applications in homeland security, IEEE Trans. Nucl. Sci. 60 (2013) 1140–1146. doi:10.1109/TNS.2013.2248166.
[15] Z. Xie, et. al., Experimental study of boron-coated straws with a neutron source, Nucl. Instruments Methods Phys. Res. Sect. A Accel. Spectrometers, Detect. Assoc. Equip. 888 (2018) 235–239. doi:10.1016/j.nima.2018.01.090.
[16] K.A. Nelson, et. al., Investigation of aerogel, saturated foam, and foil for thermal neutron detection, IEEE Nucl. Sci. Symp. Conf. Rec. (2011) 1026–1029. doi:10.1109/NSSMIC.2011.6154313.
[17] K.A. Nelson, et. al., A novel method for detecting neutrons using low density high porosity aerogel and saturated foam, Nucl. Instruments Methods Phys. Res. Sect. A Accel. Spectrometers, Detect. Assoc. Equip. 686 (2012) 100–105. doi:10.1016/j.nima.2012.04.084.
[18] N.S. Edwards, et.al., Current status of aerogel as a neutron converting material, 2015 IEEE Nucl. Sci. Symp. Med. Imaging Conf. NSS/MIC 2015. (2016) 3–6. doi:10.1109/NSSMIC.2015.7582006.

[19] D. Cester, et. al., A novel detector assembly for detecting thermal neutrons, fast neutrons and gamma rays, Nucl. Instruments Methods Phys. Res. Sect. A Accel. Spectrometers, Detect. Assoc. Equip. 830 (2016) 191–196. doi:10.1016/j.nima.2016.05.079.

[20] K.A. Guzman-Garcia, et. al., ^{10}B+ZnS(Ag) as an alternative to ^{3}He-based detectors for Radiation Portal Monitors, EPJ Web Conf. 153 (2017) 07008. doi:10.1051/epjconf/201715307008.

[21] K.A. Nelson, et. al., Investigation of a lithium foil multi-wire proportional counter for potential ^{3}He replacement, Nucl. Instruments Methods Phys. Res. Sect. A Accel. Spectrometers, Detect. Assoc. Equip. 669 (2011) 79–84. doi:10.1016/j.nima.2011.12.003.

[22] K.A. Nelson, et. al., Characterization of a mid-sized Li foil multi-wire proportional counter neutron detector, Nucl. Instruments Methods Phys. Res. Sect. A Accel. Spectrometers, Detect. Assoc. Equip. 762 (2014) 119–124. doi:10.1016/j.nima.2014.05.078.

[23] K.A. Nelson, et. al., A modular large-area lithium foil multi-wire proportional counter neutron detector, Radiat. Phys. Chem. 116 (2015) 165–169. doi:10.1016/j.radphyschem.2015.03.044.

[24] J.K. Shultis, D.S. McGregor, Design and performance considerations for perforated semiconductor thermal-neutron detectors, Nucl. Instruments Methods Phys. Res. Sect. A Accel. Spectrometers, Detect. Assoc. Equip. 606 (2009) 608–636. doi:10.1016/j.nima.2009.02.033.

[25] S.L. Bellinger, et. al., Improved high efficiency stacked microstructured neutron detectors backfilled with nanoparticle ^{6}LiF, IEEE Trans. Nucl. Sci. 59 (2012) 167–173. doi:10.1109/TNS.2011.2175749.

[26] F.D. Amaro, et. al., Novel concept for neutron detection: proportional counter filled with ^{10}B nanoparticle aerosol, Sci. Rep. 7 (2017) 41699.

[27] K.S. Mckinny, et. al., Performance optimization of systems containing boron-10 lined proportional counters, IEEE Nucl. Sci. Symp. Med. Imaging Conf. Rec. (2012) 542–546.

[28] K.S. McKinny, et. al., Optimization of coating in boron-10 lined proportional counters, IEEE Trans. Nucl. Sci. 60 (2013) 860–863. doi:10.1109/TNS.2012.2224125.

[29] Beckman Coulter Inc., LS 13 320 laser diffraction particle size analyser instrument manual, 11800, 2003.

[30] G.F. Knoll, Radiation Detection and Measurement, 4th ed., JohnWiley & Sons, New Jersey, 2000.